[TiPHOS(Rh)]$^+$: A Fortuitous Coordination Mode and an Effective Hydrosilylation Bimetallic Catalyst

Virginie Comte,* Pierre Le Gendre,* Philippe Richard, and Claude Moïse

Laboratoire de Synthèse et Electrosynthèse Organométalliques, LSEO-UMR 5188, Université de Bourgogne, Faculté des Sciences Gabriel, 6 bd Gabriel, 21000 Dijon, France

Received April 23, 2004

The reaction of the titanocene diphosphine {(η^5-C_5H_5)[η^5-C_5Me_3-1,2-(PPh_2)$_2$]$TiCl_2$} (TiPHOS; **1**) with [Rh(COD)$_2$](OTf) led to the new early−late heterobimetallic complex [(TiPHOS)Rh(COD)](OTf) (**2**), whose structure has been determined by X-ray diffraction analysis and by dynamic NMR studies. A weak bonding interaction between one of the two chloride atoms of the TiPHOS ligand and the rhodium center has been observed. The bimetallic complex **2** has been tested in parallel with the monometallic complex [(*o*-dppbe)Rh(COD)](OTf) (**3**) and has proved to be a very effective catalyst for the hydrosilylation of aromatic ketones.

Introduction

Much attention has been paid to the synthesis of early−late heterobimetallic complexes, not only for the synthetic challenge that it represents but also for the catalytic potential of these bimetallic combinations.[1] As a part of our ongoing research in this field, we have recently prepared the titanocene diphosphine **1** (TiPHOS) with a 1,2-bis(diphenylphosphino)trimethylcyclopentadienyl moiety.[2] The chelating properties of TiPHOS allowed us to synthesize three new heterobimetallic complexes. Here we describe the synthesis of the new (TiPHOS)Rh complex **2** and the investigation of its astonishing structural features with the aid of X-ray diffraction combined with dynamic NMR measurements. We also focus our attention on hydrogenation and hydrosilylation as representative reactions for comparing the activity of **2** with a monometallic analogue. Insights into the influence of the titanocene fragment on the rhodium have thus been obtained.

Results and Discussion

Treatment of [Rh(COD)$_2$](OTf) with 1 molar equiv of TiPHOS (**1**) in THF at room temperature gave the 1:1 adduct **2**, which was isolated as analytically pure brown crystals in 90% yield (Scheme 1). The $^{31}P\{^1H\}$ NMR spectrum of **2** reveals a slightly broadened doublet at 37.4 ppm with a rhodium coupling constant of 138 Hz, consistent with the coordination of both phosphorus atoms of TiPHOS to the rhodium center. The ^1H NMR spectrum of **2** shows one singlet for both lateral methyl groups bonded to the cyclopentadienyl ring, which is in accordance with the symmetric chelate structure of the TiPHOS. Signals of the COD ligand are particularly broadened, and their assignment is uncertain.

Scheme 1

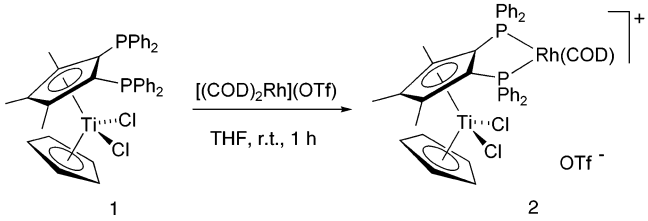

Single crystals suitable for X-ray diffraction analysis were obtained by slow diffusion of hexane into a saturated CH_2Cl_2 solution of **2**. Ortep views of the compound are shown in Figure 1 with selected bond distances and angles. The geometry of the CpCp′$TiCl_2$ fragment is typically tetrahedral with the usual structural parameters. The geometry around the rhodium is a distorted-square-planar pyramid with Cl(2) in the axial position. No differentiation is apparent in the Rh−P distances or in the Rh−C distances for the COD ligand. The Rh−Cl(2) distance of 2.74 Å is consistent with a weak bonding interaction with regard to the (μ-chloro)rhodium dimeric structures reported in the literature.[3] Additionally the Ti−Cl(2) distance of 2.3689(9) Å is somewhat longer than the Ti−Cl(1) distance of 2.3087(10) Å. This bonding interaction is also revealed by the endo position adopted by the rhodium center while being perfectly aligned with the titanium and Cl(2) atoms. Indeed, the dihedral angle defined between the P(1)−Rh−P(2) plane and the P(1)−C(28)−C(29)−P(2) plane is equal to 40°. In contrast, for the related complexes (TiPHOS)W(CO)$_4$,[2] [1,2-bis(diphenylphosphino)-3,4,5-trimethylferrocene]W(CO)$_4$,[4a] and [1,2-bis-

* To whom correspondence should be addressed. Phone: + 33 380396082. Fax: + 33 380396880. E-mail: pierre.le-gendre@u-bourgogne.fr (P.L.G.); virginie.comte@u-bourgogne.fr (V.C.).

(1) (a) Choukroun, R.; Gervais, D.; Kalck, P.; Senocq, F. *J. Organomet. Chem.* **1987**, *335*, C9. (b) Trzeciak, A. M.; Ziolkowski, J. J.; Choukroun, R. *J. Mol. Catal.* **1996**, *110*, 135. (c) Bosch, B. E.; Brümmer, I.; Kunz, K.; Erker, G.; Fröhlich, R.; Kotila, S. *Organometallics* **2000**, *19*, 1255−1261. (d) Wheatley, N.; Kalck, P. *Chem. Rev.* **1999**, *99*, 3379.

(2) Le Gendre, P.; Maubrou, E.; Blacque, O.; Boni, G.; Moïse, C. *Eur. J. Inorg. Chem.* **2001**, 1437.

(3) (a) Oro, L. A.; Carmona, D.; Garcia, M. P.; Lahoz, F. J.; Reyes, J.; Foces-Foces, C.; Cano, F. H. *J. Organomet. Chem.* **1985**, *296*, C43. (b) Pechmann, T.; Brandt, C. D.; Roger, C.; Werner, H. *Angew. Chem., Int. Ed.* **2002**, *41*, 2301.

(4) (a) Broussier, R.; Ninoreille, S.; Bourdon, C.; Blacque, O.; Ninoreille, C.; Kubicki, M. M.; Gautheron, B. *J. Organomet. Chem.* **1998**, *561*, 85. (b) Broussier, R.; Bentabet, E.; Laly, M.; Richard, P.; Kuz'mina, L. G.; Serp, P.; Wheatley, N.; Gautheron, B. *J. Organomet. Chem.* **2000**, *613*, 77.

10.1021/om040058c CCC: $30.25
Publication on Web 02/25/2005

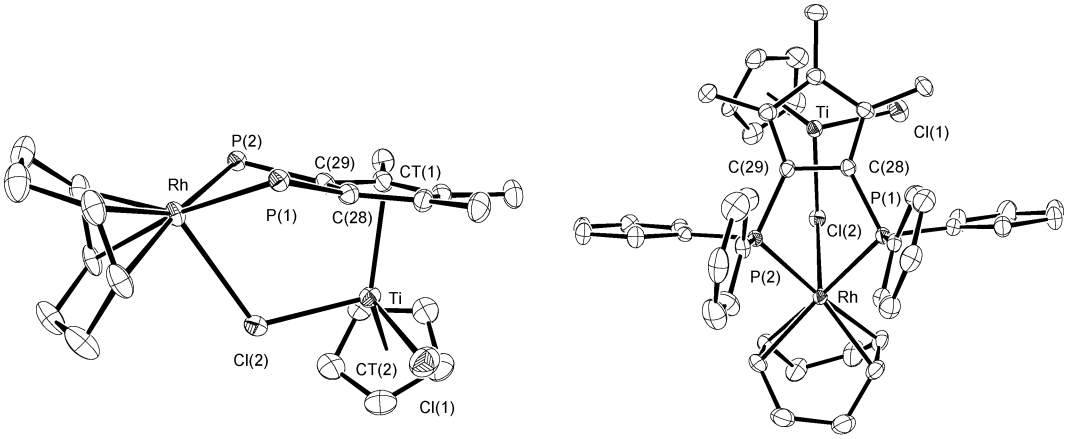

Figure 1. ORTEP views of the cationic moiety of the compound **2**, showing displacement ellipsoids at the 50% probability level. Hydrogen atoms are omitted for clarity. The phenyl groups are not shown in the front view for clarity. Selected bond distances (Å) and angles (deg): Ti−Cl(1) = 2.3087(10), Ti−Cl(2) = 2.3689(9), Ti−CT(1) = 2.118(3), Ti−CT(2) = 2.053(3), Rh−P(1) = 2.3293(8), Rh−P(2) = 2.3217(8), Rh−Cl(2) = 2.7430(8), Rh−C(38) = 2.194(3), Rh−C(39) = 2.219(3), Rh−C(42) = 2.206(3), Rh−C(43) = 2.207(3), C(38)−C(39) = 1.384(5), C(42)−C(43) = 1.390(5); Cl(1)−Ti−Cl(2) = 94.21(4), CT(1)−Ti−CT(2) = 131.27(13), Ti−Cl(2)−Rh = 114.46(3), P(1)−Rh−P(2) = 81.14(3), C(28)−P(1)−Rh = 103.67(10), C(29)−P(2)−Rh = 104.02(10).

(diphenylphosphino)-3,4,5-trimethylferrocene]$PdCl_2$[4b] the dihedral angles described as above are close to 0°.

Since the ability of the TiPHOS ligand to adopt a tridentate (P, P, Cl) coordination mode in the solid state is established, it appears clearly that the titanium atom is chiral and the environment around the rhodium is asymmetric. Nevertheless, NMR data collected at room temperature were consistent with a symmetric chelate structure. To elucidate this contradiction, we measured NMR spectra of **2** at lower temperatures (Figure 2).

At 273 K, the $^{31}P\{^1H\}$ NMR spectrum of **2** reveals a single set of eight signals with an ABX pattern (J(P−P) = 27 Hz and J(P−Rh) = 138 Hz). The NMR evolution vs temperature is reversible, since when the temperature is raised back, the $^{31}P\{^1H\}$ NMR spectrum again exhibits a doublet. The NMR behavior of **2** is thus consistent with the weak coordination of one of the two chloride atoms to the rhodium with an accompanying dynamic exchange process (Figure 3). At this point it is worth mentioning that a quite similar process has been recently described by Bookham et al. for rhodium complexes with diphosphines bearing pendant pyridyl donor groups.[5] The higher temperature range in their case (between 308 and 373 K) is in accordance with a stronger N-coordination to the Rh in comparison to the weak Rh−Cl interaction we describe therein.

Nevertheless, the evolution of the NMR spectra below 273 K remains a particularity of our system. Indeed, from this temperature the dynamic exchange becomes slow with respect to the NMR time scale and there is a parallel increase in the gap of the phosphorus chemical shifts. As can be seen in Figure 4, a downfield shift of 0.8 ppm for one phosphorus resonance (P′) and a upfield shift of 0.2 ppm for the other (P) are raised at 213 K. The coupling constant between both phosphorus atoms remaining equal to 27 Hz, the ABX spectrum becomes an AMX spectrum as the temperature decreases. Thus, each phosphorus atom, one being confined between both chloride atoms and the other being beside them, has its own magnetic environment which slightly and independently changes.

We suggest that the rigidity of the TiPHOS ligand, reinforced by the interaction of the rhodium with chloride atoms, is at the origin of this phenomenon. The corresponding gNMR simulated spectra reported as lower traces in Figure 2 have been fitted to a ABX spin system where A, B = ^{31}P and X = ^{103}Rh, taking into account an interchange and a variation of the phosphorus environment. An Eyring plot of ln(k/T) vs $1/T$ (273 K < T < 303 K), using the rate constants k calculated from the simulation, gives an enthalpy of activation ΔH = 56(±3) kJ mol^{-1}, which is in agreement with a weak Rh−Cl interaction. To see if the dynamic NMR behavior of **2** is reliable, we performed a variable-temperature NMR study at higher frequency (500 MHz instead of 300 MHz NMR spectrometer). The NMR data were very similar, with the AB part of the system less marked and dissymmetric at 233 K, as illustrated in Figure 5. It is noteworthy that this exchange process does not involve an additional participation of CD_2Cl_2, since the patterns of the spectra are similar in CD_3OD. Finally, analogous features are observed in the ^1H NMR spectra.

To evaluate the effect of the titanocene fragment on the catalytic activity of the rhodium center in the bimetallic system **2**, we have synthesized and tested in parallel the monometallic rhodium complex **3** with 1,2-bis(diphenylphosphino)benzene, whose rigidity and chelate structure are comparable to those of TiPHOS. [(*o*-dppbe)Rh(COD)](OTf) (**3**) was prepared by the reaction of [Rh(COD)$_2$](OTf) with 1,2-bis(diphenylphosphino)-benzene, as described in the literature.[6] Rhodium−diphosphine complexes have been known for many years to be effective catalysts in the hydrogenation of olefins and ketones.[7] Therefore, we carried out the catalytic hydrogenation of the standard test substrate methyl α-acetamido cinnamate in methanol, at 8 bar of hydrogen pressure and using 1 mol % of **2** or **3**. With the aim of comparing the activities of both systems, we stopped

(5) Bookham, J. L.; Smithies, D. M.; Pett, M. T. *Dalton* **2000**, 975.

(6) Murakami, M.; Itami, K.; Ito, Y. *Organometallics* **1999**, *18*, 1326.

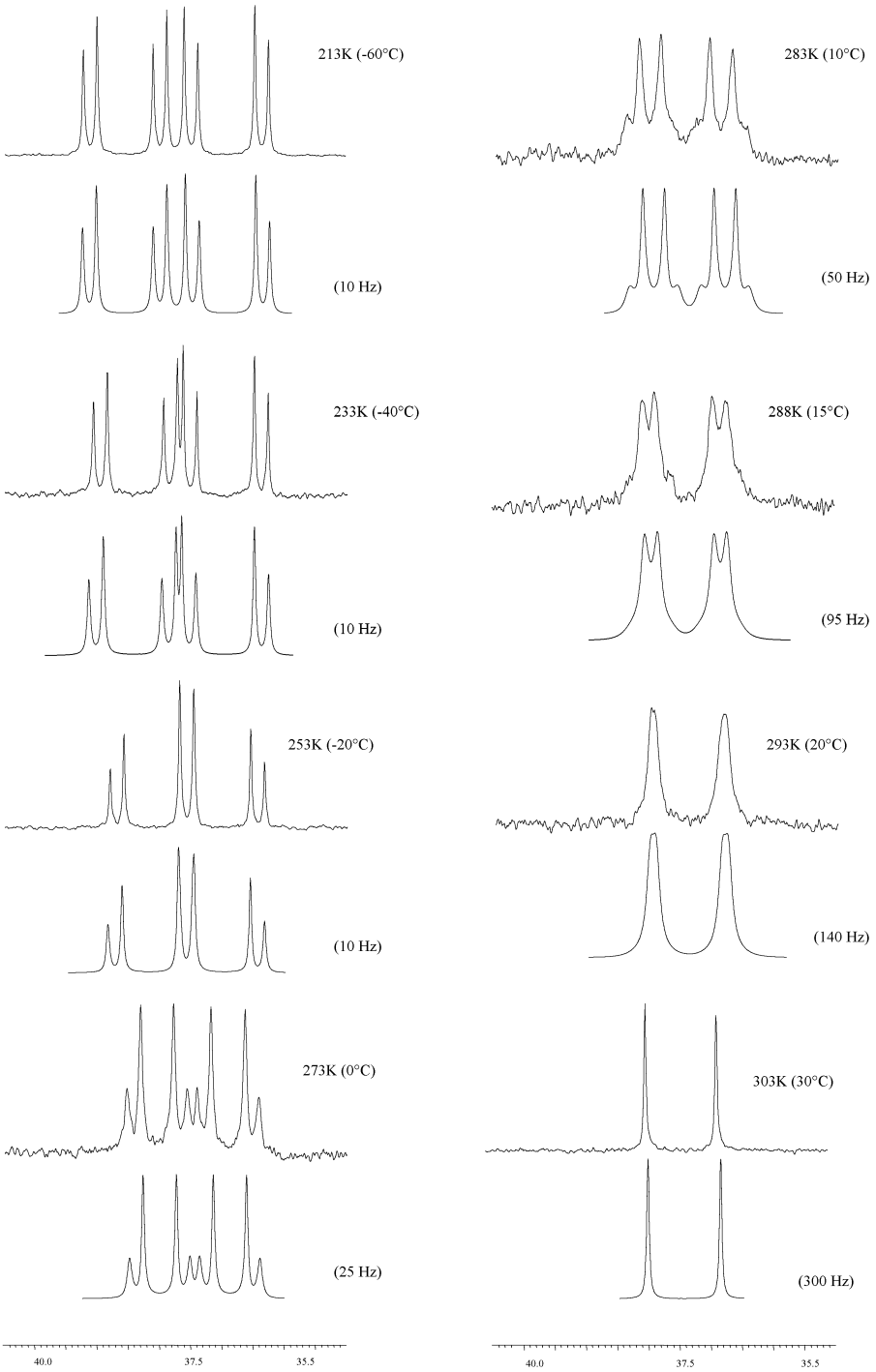

Figure 2. (upper traces) $^{31}P\{^{1}H\}$ NMR spectra of **2** at selected temperatures (CD_2Cl_2, 300 MHz). (lower traces) Computer-simulated spectra using gNMR (calculated exchange rates ($1/\tau$) are shown in parentheses).

the reaction after only 1 h and measured the conversion by ^{1}H NMR on the crude reaction mixture. Unfortunately, the bimetallic complex **2** appeared to be less active than the monometallic complex **3** (35% and 90% conversion, respectively). To avoid the eventual coordination of methanol to the titanium center, which could prevent the latter from interacting with the substrate, we tested the hydrogenation in CH_2Cl_2. In contrast, the bimetallic system appeared inactive in this solvent. Hydrogenation of ketones gave comparable results. Thus, the hydrogenation of acetophenone in methanol at 55 °C and 60 bar of hydrogen pressure in the presence of 1 mol % of the monometallic complex **3** led to 35% yield after 24 h, whereas only 8% of phenylethanol is obtained with **2** under these conditions. All these results show a disadvantage of the bimetallic system over the mononuclear rhodium catalyst for hydrogenation reactions.

(7) (a) Börner, A.; Holz, J.; Burk, M. J.; Bienewald, F. In *Transition Metals for Organic Synthesis*; Beller, M., Bolm, C., Eds.; Wiley-VCH: Weinheim, Germany, and New York, 1998; Vol. 2. (b) Ohkuma, T.; Noyori, R. In *Transition Metals for Organic Synthesis*; Beller, M., Bolm, C., Eds.; Wiley-VCH: Weinheim, Germany, and New York, 1998; Vol. 2. (c) Noyori, R. In *Asymmetric Catalysis in Organic Synthesis*; Wiley: New York, 1994.

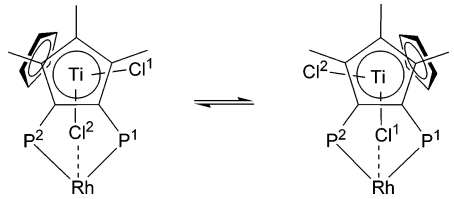

Figure 3. Dynamic exchange of the two phosphorus environments.

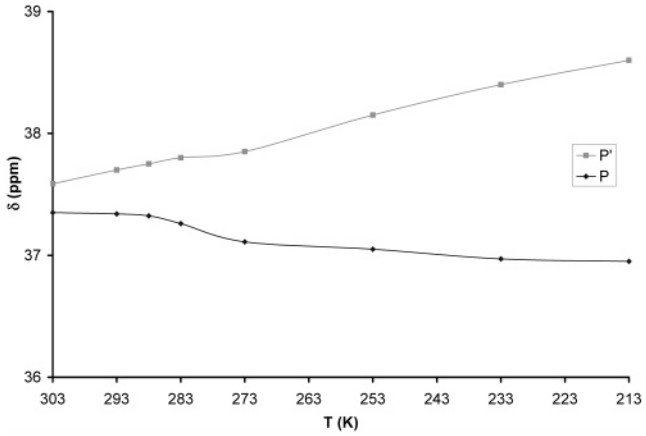

Figure 4. Evolution of the phosphorus chemical shifts vs temperature.

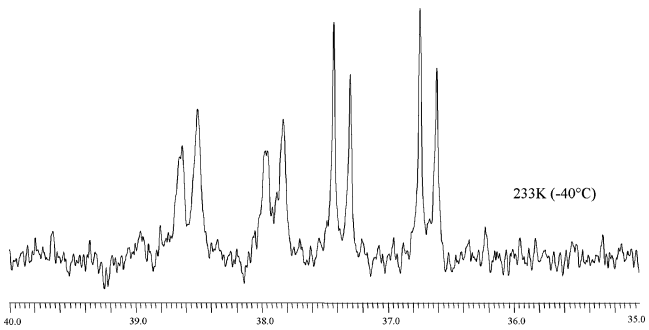

Figure 5. $^{31}P\{^1H\}$ NMR spectrum of **2** at 233 K recorded on a 500 MHz NMR spectrometer (solvent CD_2Cl_2).

Considering that both rhodium diphosphine and titanium complexes[7c,8,9] catalyze the hydrosilylation reaction, we continued our effort to explore the catalytic ability of **2** in this reaction. At first, we focused our study on the hydrosilylation of acetophenone and the results are summarized in Table 1. Acetophenone is allowed to react for 5 h at room temperature with dihydrodiphenylsilane in THF in the presence of 0.1 mol % of catalyst. With this substrate, the more active catalyst is found to be the bimetallic complex **2**. After hydrolysis and treatment, phenylethanol is then obtained with a conversion of 62% (Table 1, entry 1), while with the monometallic rhodium complex **3** only 36% of conversion is observed (entry 2). Despite the fact that comparison

Table 1. Catalytic Hydrosilylation of Acetophenone[a]

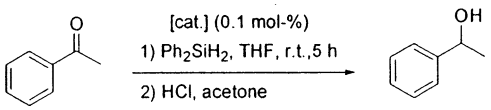

entry	catalyst	yield, %[b]
1	[(TiPHOS)Rh(COD)]OTf (**2**)	62
2	[(*o*-dppbe)Rh(COD)]OTf (**3**)	36
3	Cp_2TiCl_2[c]	0
4	**3** + Cp_2TiCl_2[d]	41
5	**3**[e]	34

[a] Conditions: acetophenone (2.2 mmol), Ph_2SiH_2 (2.4 mmol), THF (2 mL), catalyst (0.1 mol-%), 5 h. [b] Determinated by ^1H NMR on the crude reaction mixture after hydrolysis. [c] The reaction was carried out with 1 mol % of Cp_2TiCl_2. [d] The reaction was carried out with 0.1 mol % of **3** and 0.5 mol % of Cp_2TiCl_2. [e] The reaction was performed in CH_2Cl_2.

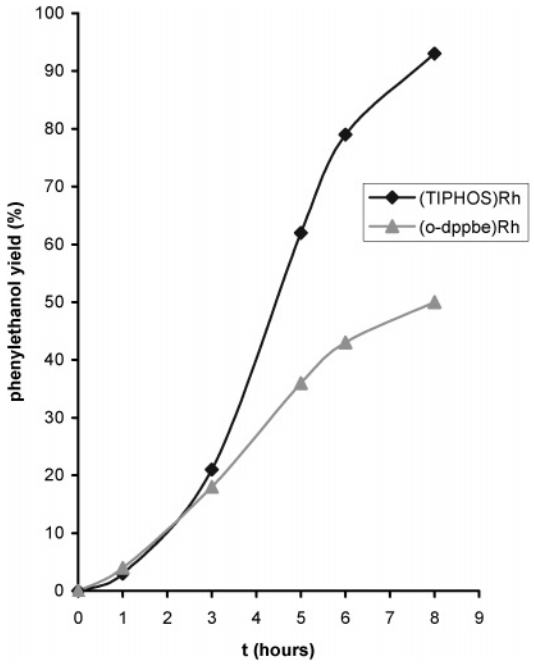

Figure 6. Conversion in phenylethanol vs time (reaction conditions as in Table 1).

with other diphosphine−rhodium complexes reported in the literature is complicated (catalytic conditions are always different), it appears that the bimetallic complex **2** we described is competitive.[8]

The better activity of the bimetallic complex **2** in comparison to **3** was confirmed by following the kinetics of the reaction with both complexes over 8 h (Figure 6). Indeed, a turnover frequency of 205 h^{-1} is reached with **2**, whereas **3** gives only a TOF of 90 h^{-1}. According to the currently accepted mechanism, the species starting the hydrosilylation process is the low-valence rhodium complex $[Rh(diphosphine)]^+$.[7c] Therefore, the induction period observed with the bimetallic complex **2** might be explained by the fact that **2** releases the COD ligand more slowly than **3**. At this point we should mention that the presence of COD in the medium has been confirmed by GC MS in both cases.

Since the fragment Cp_2TiCl_2 within the bimetallic complex **2** is a priori able to activate the ketone toward the Rh−Si bond, we carried out the hydrosilylation of acetophenone with **3** with an additional substoichio-

(8) (a) Marciniec, B.; Gulinski, J.; Urbaniak, W.; Kornetka, R. W. In *Comprehensive Handbook on Hydrosilylation*; Marciniec, B., Ed.; Pergamon: New York, 1992. (b) Brunner, H. In *Transition Metals for Organic Synthesis*; Beller, M.; Bolm, C., Eds.; Wiley-VCH: Weinheim, Germany, and New York, 1998; Vol. 2.

(9) (a) Yun, J.; Buchwald, S. L. *J. Am. Chem. Soc.* **1999**, *121*, 5640. (b) Carter, M. B.; Schiøtt, B.; Gutierrez, A.; Buchwald, S. L. *J. Am. Chem. Soc.* **1994**, *116*, 11667. (c) Halterman, R. L.; Ramsey, T. M.; Chen, Z. *J. Org. Chem.* **1994**, *59*, 2642. (d) Xin, S.; Harrod, J. F. *Can. J. Chem.* **1995**, *73*, 999. (e) Imma, H.; Mori, M.; Nakai, T. *Synlett* **1996**, 1229. (f) Rahimian, K.; Harrod, J. F. *Inorg. Chim. Acta* **1998**, *270*, 330.

Table 2. Hydrosilylation of Propiophenone and α-Tetralone Catalyzed by 2 or 3[a]

entry	substrate	catalyst	yield,[b] %
1	propiophenone	[(TiPHOS)Rh(COD)]OTf (**2**)	32
2	propiophenone	[(*o*-dppbe)Rh(COD)]OTf (**3**)	22
3	α-tetralone	**2**	72
4	α-tetralone	**3**	40

[a] Conditions: ketone (2.2 mmol), Ph_2SiH_2 (2.4 mmol), THF (2 mL), catalyst (0.1 mol %), 5 h. [b] Determinated by ^1H NMR on the crude reaction mixture after hydrolysis.

metric amount of Cp_2TiCl_2. Under these conditions, the yield of phenylethanol was only slightly improved. Additionally, it is worth mentioning that Cp_2TiCl_2 does not catalyze the hydrosilylation of acetophenone under these conditions (Table 1, entry 3). Therefore, it can be assumed that both metallic fragments should be tethered to exhibit a significant cooperative effect. The early-metal fragment in **2** can also be seen as a chloro ligand able to stabilize the low-valence rhodium intermediate species. We thus examined whether a chlorinated solvent could improve the catalytic performance of **3**. The hydrosilylation of acetophenone in CH_2Cl_2 with a catalytic amount of the complex **3** afforded phenylethanol in the same yield as in THF (entry 5). Nevertheless, this result should be considered with caution with regard to the coordination mode of the TiPHOS ligand. Indeed, the structural constraints of TiPHOS impose a facial coordination of the two phosphorus atoms and of one of the two chloride atoms to the rhodium center, a coordination scheme which is very difficult to mimic by just adding a chloro ligand to a monometallic diphosphine−rhodium complex. At this point in our study, we cannot distinguish whether this is a bimetallic or a multidentate ligand effect. However, it is obvious that the chloride bridge reinforces the link between both metals and allows them to interact more easily.

These results prompted us to extend this comparative study to other ketones. We thus carried out the hydrosilylation of propiophenone and α-tetralone under conditions similar to those for acetophenone. In both cases the bimetallic complex **2** leads to better yields than its monometallic analogue **3**, with a particularly remarkable gap of 32% yield in the case of α-tetralone (Table 2).

Although hydrogenation and hydrosilylation of ketones are closely related catalytic reactions, it appears that the TiPHOS ligand within the same rhodium complex gives opposite results. This apparent inconsistency might be first explained by considering the mechanism of the selected reactions. For the hydrogenation of ketones, the mechanism involves the insertion of the carbonyl group into a Rh^I-H bond, giving Rh−O and C−H bonds.[7c] On the other hand, for the hydrosilylation, this insertion takes place into a $Rh^{III}-Si$ bond to form Rh−C and Si−O bonds. The affinity of titanium for oxygen can thus either interfere or assist the activity of the rhodium center. Moreover, TiPHOS, which is revealed to be a tridentate ligand, can through the coordination of its chloride atom poison or, in contrast, stabilize catalytically active species.

Conclusion

We have described the synthesis and the characterization of the new Ti−Rh early-late bimetallic complex **2**. An X-ray diffraction study has revealed a weak bonding interaction between one of the two chloride atoms of TiPHOS with the rhodium center. NMR studies confirm these structural features with an accompanying dynamic exchange in solution.

Application of this system in the hydrosilylation of aromatic ketones has shown its effectiveness with regard to a monometallic rhodium complex. These preliminary results make TiPHOS an attractive ligand to explore the coordinative mode of the phosphine metallocene dichloride and the catalysis by early−late complexes. Further studies concerning the synthesis and application of TiPHOS possessing planar chirality are in progress.

Table 3. Crystal Data and Structure Refinement Details for 2

formula	$C_{45}H_{46}P_2Cl_2TiRh\cdot CH_2Cl_2\cdot CF_3SO_3$
M_r	1104.46
T, K	110(2)
cryst syst	triclinic
space group	
a, Å	10.8126(2)
b, Å	12.8632(3)
c, Å	16.3188(3)
α, deg	87.923(1)
β, deg	84.071(2)
γ, deg	84.539(1)
V, Å^3	2246.51(8)
Z	2
F(000)	1124
D_{calcd}, g/cm^3	1.633
diffractometer	Enraf-Nonius KappaCCD
scan type	mixture of ϕ rotations and ω scans
λ, Å	0.710 73
μ, mm^{-1}	0.956
cryst size, mm^3	0.28 × 0.21 × 0.08
max (sin θ)/λ, Å^{-1}	0.65
index ranges	
h	−14 to +14
k	−16 to +16
l	−14 to +21
abs cor	SCALEPACK
no. of rflns collected (RC)	16 888
no. of indep RC (IRC)	(R(int) = 0.0264)
IRCGT = IRC with $I > 2\sigma(I)$	8055
refinement method	full-matrix least squares on F^2
no. of data/restraints/params	10 164/0/560
R for IRCGT	R1[a] = 0.0435, wR2[b] = 0.1097
R for IRC	R1[a] = 0.0613, wR2[b] = 0.1186
goodness of fit[c]	1.041
largest diff peak and hole, e Å^{-3}	0.705 and −0.854

[a] $R1 = \Sigma(||F_o| - |F_c||)/\Sigma|F_o|$. [b] $wR2 = [\Sigma w(F_o^2 - F_c^2)^2/\Sigma[w(F_o^2)^2]^{1/2}$, where $w = 1/[\sigma^2(F_o^2) + 2.43P + (0.057P)^2]$ and $P = (\mathrm{Max}(F_o^2, 0) + 2F_c^2)/3$. [c] Goodness of fit $= [\Sigma w(F_o^2 - F_c^2)^2/(N_o - N_v)]^{1/2}$.

Experimental Section

All reactions were carried out under an atmosphere of purified argon using vacuum line techniques. Solvents were dried and distilled under argon from sodium and benzophenone before use. Elemental analyses were performed on a EA 1108 CHNS-O FISONS instrument. ^1H and ^{31}P NMR spectra were recorded on Bruker 300 MHz Avance and Bruker 500 MHz Avance spectrometers. Chemical shifts are denoted in ppm (δ) relative to TMS (^1H) or external H_3PO_4 (^{31}P). Coupling constants are reported in Hz. The TiPHOS ligand[2] and [(*o*-dppbe)Rh(COD)](OTf) (COD = 1,5-cyclooctadiene)[6] were prepared as described.

Preparation of [(TiPHOS)Rh(COD)](OTf). To a solution of [Rh(COD)$_2$](OTf) (106 mg, 0.22 mmol) in THF (4 mL) at

room temperature was added a solution of TiPHOS (149 mg, 0.22 mmol) in THF (2 mL). The reaction mixture was stirred for 1 h, filtered, and then concentrated to ca. 2 mL under vacuum. Hexane (4 mL) was added to the solution and left at room temperature until crystallization appeared complete. The crude product was recrystallized from dichloromethane−hexane to give brown crystals (202 mg, 90% yield). ^{1}H NMR (CD_2Cl_2, 295 K): δ 7.80−7.00 (m, 19H, Ph), 6.60 (broadened signal, 1H, Ph), 6.19 (s, 5H, Cp), 5.20 (broadened signal, 1H, C*H* COD), 4.80−4.10 (m, 3H, C*H* COD), 2.90−2.0 (m, 8H, CH_2 COD), 2.08 (s, 6H, CH_3), 1.80 (s, 3H, CH_3). ^{31}P{^{1}H} NMR (CD_2Cl_2, 298 K): δ 37.4 (d, $^1J_{PRh}$ = 138 Hz). ^{1}H NMR (CD_2Cl_2, 213 K): δ 8.14−6.57 (m, 18H, Ph), 6.57 (m, 1H, Ph), 6.11 (s, 5H, Cp), 5.60 (m, 1H, Ph), 5.23 (m, 1H, C*H* COD), 4.49 (m, 2H, C*H* COD), 4.09 (m, 1H, C*H* COD), 2.69−1.98 (m, 8H, CH_2 COD), 2.04 (s, 3H, CH_3), 1.99 (s, 3H, CH_3), 1.71 (s, 3H, CH_3). ^{31}P{^{1}H} NMR (CD_2Cl_2, 213 K): δ 38.6 (dd, $^2J_{PP}$ = 27 Hz, $^1J_{PRh}$ = 138 Hz), 36.9 (dd, $^2J_{PP}$ = 27 Hz, $^1J_{PRh}$ = 138 Hz). Anal. Calcd for $C_{46}H_{46}O_3Cl_2F_3SP_2TiRh$: C, 54.14; H, 4.55; S, 3.14. Found: C 54.05; H, 4.32; S, 2.89.

Hydrogenation Procedure. (a) For Methyl α-Acetamido Cinnamate. An autoclave was loaded under argon with catalyst (6.2×10^{-3} mmol, 1 mol %), substrate (0.62 mmol), and 10 mL of freshly distilled solvent. The argon atmosphere was replaced by hydrogen, and the hydrogenation was performed at room temperature under 8−9 bar of hydrogen for 1 h. Conversion was checked by ^{1}H NMR measurements on the crude product.

(b) For Ketones. An autoclave was loaded under argon with catalyst (0.0125 mmol; 1 mol %), freshly distilled methanol (5 mL), acetophenone (1.25 mmol), and distilled triethylamine (0.625 mmol; C = 0.25 M). The argon atmosphere was replaced by hydrogen, the initial pressure was set to 60 bar, and the reaction mixture was stirred for 24 h at 50−55 °C. Conversion was checked by ^{1}H NMR measurements of the crude product.

Hydrosilylation Procedure. All the reactions were conducted under an argon atmosphere in 10 mL Schlenk flasks connected to a vacuum line and fitted with a rubber septum. To a solution of the catalyst (2.2×10^{-3} mmol; 0.1 mol %) in THF (2 mL) were added Ph_2SiH_2 (2.4 mmol) and ketone (2.2 mmol). The mixture was then stirred at room temperature for 5 h or more. The solution was then quenched with 15 mL of a 6:1 acetone−10% aqueous HCl mixture and stirred for 1 h. After neutralization with saturated $NaHCO_3$, the phases were separated and the aqueous layer was extracted three times with 25 mL of CH_2Cl_2. The combined organic phases were dried, filtered, and evaporated under vacuum. The absolute yields of the products and the amounts of residual reactants in the final reaction mixtures were determined by ^{1}H NMR spectroscopy.

Crystallographic Data. A single crystal of **2** was obtained from dichloromethane/hexane solution. Intensities were collected on an Enraf-Nonius Kappa CCD diffractometer at 110 K using Mo Kα radiation. The structure was solved via a Patterson search program[10] and refined with full-matrix least-squares methods[10] based on $|F^2|$ with the aid of the WinGX program.[11] All non-hydrogen atoms were refined with anisotropic thermal parameters. Hydrogen atoms were included with a riding model with isotropic temperature factors fixed to 1.2 times (1.5 for methyl groups) those of the corresponding parent atoms. Crystal data are reported in Table 3.

Acknowledgment. We wish to thank Dr. M. Picquet for helpful discussions, assistance in NMR experiments and gNMR simulation. Although ^{103}Rh NMR measurements were unsuccessful, thanks are due to Dr. R. Thouvenot (University Paris VI) for his efforts.

Supporting Information Available: Tables giving detailed information on the X-ray crystal structure analyses of **2**. This material is available free of charge via the Internet at http://pubs.acs.org.

OM040058C

(10) Sheldrick, G. M. SHELXL97 and SHELXS97; University of Göttingen, Göttingen, Germany, 1997.
(11) Farrugia, L. J. *J. Appl. Crystallogr.* **1999**, *32*, 837.